Phendione-Transition Metal Complexes with Bipolar Redox for Lithium Batteries

Alae Eddine Lakraychi, Simon De Kreijger, Deepak Gupta, Benjamin Elias and Alexandru Vlad*

Institute of Condensed Matter and Nanosciences, Molecular Chemistry, Materials and Catalysis Division (IMCN/MOST), Université Catholique de Louvain, Place Louis Pasteur 1, Louvain-la-Neuve, Belgium.
E-mail: alexandru.vlad@uclouvain.be

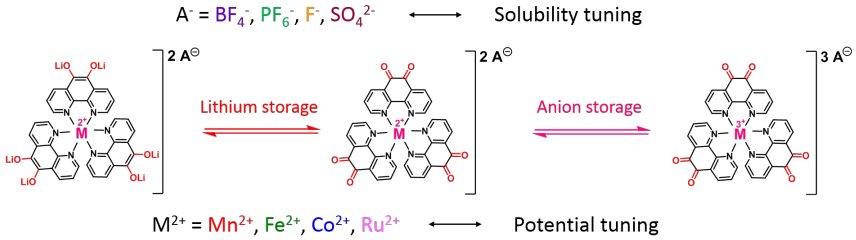

***7**-electrons charge storage via the bipolar redox in Phendione - transition metal complexes is reported. TM and counter anion chemistry are found to largely tune the redox potential and cycling stability.*

Abstract: *1,10-Phenanthroline-5,6-dione (Phendione) - based transition metal complexes are known for their use in pharmacological and catalysis applications. However, their application in electrochemical energy storage has not been investigated thus far. Herein we prove the feasibility of employing phendione - transition metal complexes for electrochemical charge storage by taking advantage of the reversible redox of both, carbonyl groups and transition metal center, contributing thus to augmented charge storage. Interestingly, the chemistry of the counter ion in the studied complexes effectively tunes the solubility and improves the cycling stability. Whereas further studies are required to limit the solubility and active species shuttle, this study explores the bottlenecks of phendione - transition metal complexes as electrode materials for solid electrode format batteries.*

Quinone derivatives constitute an important class of naturally occurring compounds found in plants, fungi and bacteria, with important role as charge transfer mediators in photosynthesis and respiratory chain in chloroplasts and mitochondria (plastoquinones and ubiquinones).[1] The redox activity of quinones is also well-established in molecular electrochemistry,[2] with interesting characteristics manifested by multi-electron redox reaction and fast kinetics. Owing to these properties, quinone derivatives have attracted vivid interest in the electrochemical charge storage research community. The first mention for use of quinones as active material in batteries can be traced back to 1972, when Alt *et al.* reported the use of simple benzoquinone as electrode material for lithium storage. The cell provided an output voltage of 2.50 V vs. Li^+/Li for a theoretical capacity of 496 $mAh.g^{-1}$ with an energy density as high as $1kWh.g^{-1}$.[3] Since then, many different molecular designs have been proposed,[4] with the use of quinone derivatives in many forms in order to fit with the desired energy storage device requirements. So far, quinones have been used as dissolved or bulky solid active material, but also in different molecular architectures such as small molecules (mainly in oxidized but also in reduced state – metal-reservoir cathode), polymers or hybrid frameworks.

Quinone-based small molecules are usually privileged owing to their higher energy density and easier structural flexibility. Indeed, their redox potential can be effectively modified by incorporating electron withdrawing or donating groups.[5] Along the same principles, fusing with hetero-aromatic rings[6] or switching the isomery to foster electrostatic interaction [7] was also shown positive shift of the redox potential. Whereas redox potential increase brings higher energy density metrics, cycling stability is still of major concerns when integrating quinone derivatives in lithium cells. Indeed, solubility remains a topic of concern when dealing with small molecules, requiring various approaches to be applied. For example, integration of ionic groups ($-CO_2Li$, $-SO_3Li$)[5a, 8] or H-bond donor groups ($-NH_2$)[9] makes these less soluble in conventional battery electrolytes, and thus suitable for stationary batteries. Another effective approaches can be broadly resumed to polymerization (or polycondensation) of quinone derivatives[10] or impregnation/grafting in/onto mesoporous carbon or conductive supports.[11] The later, in addition, can lead to competitive power performances given the electron-conducting framework provided. Covalent or Metal Organic Frameworks (COFs/MOFs) have been also considered and found efficient to address the solubility issues,[12] accompanied with a real possibility to enhance the intrinsic ionic conductivity (anion, cation, solvent molecule diffusion).

Recent studies suggest that metal organic complexes (MOCs) are potential candidates for efficient electrochemical energy storage.[13] Fichtner *et al.,* have reported the use of Cu-porphyrin complex as both positive and negative electrode material, combining high storage capacity and rate capability as well as extended cycling stability.[13b] By synergizing the concept of both Li-ion and redox flow batteries, $[Fe(bipyridine)_3](BF_4)_2$ complex showed promising electrochemical performances as high voltage catholyte material for lithium storage.[13c] Along the same lines, 10-Phenanthroline-5,6-dione (Phendione, hereafter denoted as Phendi) was used to form stable MOCs by chelating with a large variety of transition metals (TM) through N atoms.[14]

These Phendi-complexes have been a subject of interest in catalysis and pharmacological applications thanks to their electrochemical and biomedical properties, respectively.[15] To be noted that Phendi ligand was also used as active material in lithium batteries, with a reversible lithium storage (corresponding to two Li^+) at an average redox potential of 2.74 V vs. Li^+/Li, yet suffering from major solubility issues.[16] An extended analysis of the redox behavior of Phendi-based complexes was reported by Abruna *et al.*,[17] disclosing the reversible molecular electrochemistry for both, transition metal and ligands. However, to the best of our knowledge, the charge storage performance of Phendi-based complexes in the solid phase is not yet documented.

Herein, we prove the feasibility of electrochemical charge storage for a series of Phendione-transition metal (Phendi-TM) complexes, in the conventional, solid form cells. The impact on the redox potential and cycling stability of different TM cations (Mn^{2+}, Fe^{2+}, Co^{2+} and Ru^{2+}) as well as the counter anions (BF_4^-, PF_6^-, F^- and SO_4^{2-}) is analyzed and discussed. In a single redox cycle, Phendi-TM complexes are able to reversibly store not only Li cations through the redox of carbonyl groups at the Phendi ligand center, but also at the anions, thanks to the reversible redox of TM, leading to a new multi-electron bipolar redox system (Scheme 1).[18]

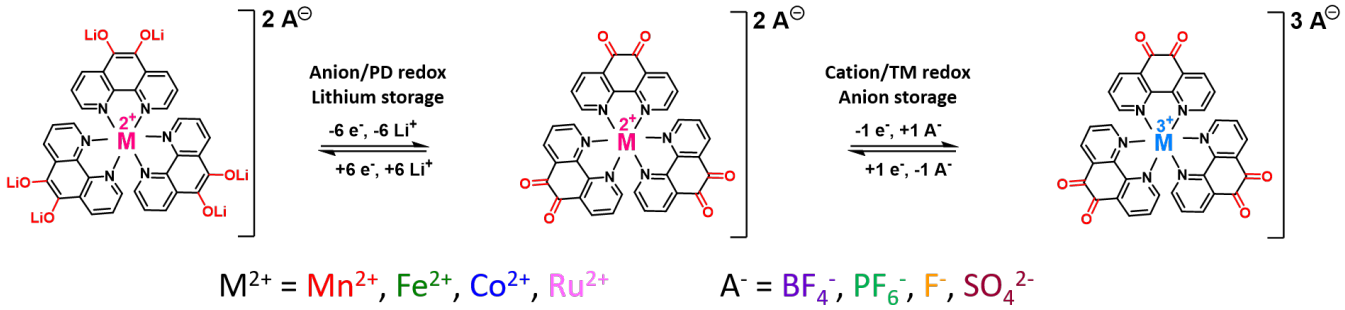

Scheme 1. Multi-electron bipolar redox in 1,10-Phenanthroline-5,6-dione - transition metal complex $[TM(Phendi)_3]\bullet xA$. Center: pristine, as-synthesized redox state. To compensate the charge neutrality, anions are part of the molecular structure. Left side process: Li cation storage involving the *n*-type redox of carbonyl groups. Right side process: the TM *p*-type redox can be accessed at higher potential, and operates through anion charge compensation.

The synthesis of Phendi-TM complexes was adapted from Abruna *et al.*[17] In brief, an aqueous solution of metal salt is added to 3.3 equivalents of Phendi ligand dissolved in ethanol (refer to Experimental Section and SI for specific synthesis and process details). After 12 hours of reaction at room temperature, the complexes were recovered by precipitation using a saturated aqueous solution of NH_4PF_6. The composition of the studied complexes was confirmed by Fourier-transmission infrared spectroscopy (FTIR), nuclear magnetic resonance (NMR) spectroscopy, thermal analysis and X-ray diffraction.

The complexation is first of all evidenced by the blueshift of the carbonyl (C=O) band from 1681 cm^{-1} for free Phendi, to higher frequencies for complexed Phendi. This can be explained by the electron density variation on the Phendi ligand upon coordination with metal-ion (Figure 1-a).[19] The observed blueshift establishes the fact that the ligands are exclusively N,N'-coordinated, unlike O,O'-coordination where the carbonyls have been shown to undergo a redshift of about 200-300 cm^{-1}.[20] The complex formation is further confirmed by the presence of a strong band at 848 cm^{-1} which is assigned to ν(P-F) indicating the presence of the PF_6^- counter ions in the synthesized solids.[17] The ^{13}C NMR data corroborate the IR analysis, with a deshielding observed on all aromatic carbons, accompanied by a noticeable chemical shift of C=O from 180 ppm to ~175 ppm (Fig. S1-b). Thermogravimetric analysis confirms no residual or crystalline solvent molecules whereas X-ray diffraction indicates that all obtained complexes are crystalline in nature (Fig. S2 and S3).

The overlaid FTIR spectra of all studied complexes show that the ν(C=O) frequency is sensitive to the chemical nature of TM cation. Indeed, when Mn^{2+} is used, the ν(C=O) stretching band appears at 1691 cm^{-1} instead of ~1701 cm^{-1} observed with all other TMs. Moreover, the substitution of Fe^{2+} with Ru^{2+} in the complex involves a strong deshielding of all proton signals (Fig. S1-a). The deshielding effect is more pronounced on protons in *para* position (with respect to N coordinating atom, H_3), since the other protons (i.e., H_1 *in ortho* or H_2 in *meta* position with respect to N coordinating atom) are to be found above the shielding zone neighboring heteroaromatic rings.[21] These observations confirm the influence of the ionic potential of TM on the electron density distribution within Phendi ligand.

Prior to investigation of lithium storage performances in solid-phase, we have first analyzed the molecular redox response of the Phendi-TM complexes by performing cyclic voltammetry analysis of dissolved species. The Phendi based redox processes were observed in a reversible manner at distinct potentials. Basically, the electroactivity of quinones is evolving between three reversible redox states, fully oxidized quinone (Q) that can be reduced first to an intermediate semi-quinone radical anion ($Q^{\bullet}$-), to then a fully reduced quinol (Q^{2-}). The electrochemical response of free Phendi shows two reversible, one-electron redox waves centered around -1.70 and -0.75 V vs. Ag/Ag^+ (Figure 1-b). Comparatively, all Phendi-TM complexes display qualitatively similar electrochemical behavior to that recorded for free Phendi (Figure 1-c).

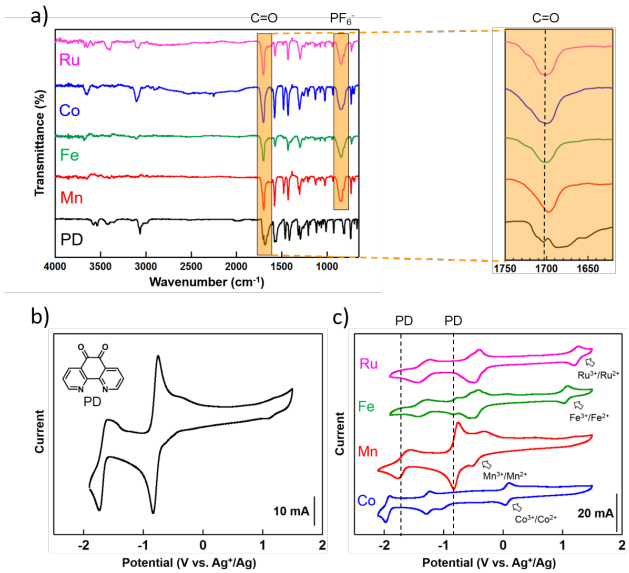

Figure 1. Spectroscopic and electrochemical analysis of Phendi and Phendi-TM complexes. a) Overlaid FTIR spectra of Phendi (black) and Phendi-TM complexes with Mn (red), Fe (green), Co (blue) and Ru (pink) metal centers. Inset – close up on the carbonyl stretching band. Cyclic voltammetry (CV) for 0.5 mM of Phendi at glassy carbon electrode (b) and Phendi-TM complexes at platinum electrode (c) in 0.1M $[NBu_4][ClO_4]$ acetonitrile solution, all data acquired at a scan rate of 100 $mV.s^{-1}$.

As mentioned earlier, for a given disubstituted quinone, the electronic effect of the substituents can have a significant impact on the redox potential values. In this regard, Jouhara *et al.,* have pointed out that the donor inductive effect (+I) of carboxylate substituent ($-COO^-$) can be mitigated by simple cationic substitution, and thus alter the redox potential of carboxyphenolate ligands.[22] The authors have observed a quasi-linear correlation between the redox potential and the ionic potential of the metal cation. A similar effect can be also noticed in the series of complexes studied in this work. In all $[TM(Phendi)_3]•2PF_6$ complexes, a noticeable redox potential shift of the ligands (as compared to free Phendi) was detected. TMs with higher ionic potential (namely Ru^{2+} and Fe^{2+}) induces a redox potential shift to higher values, whereas the shift is less pronounced in the case of Mn^{2+} (possessing the lowest ionic potential among the TMs used in this study). The use of Co^{2+} leads to a negative potential shift of the ligand which requires further analysis to understand the origin of this non-trivial response. Overall, the chelation is also shown here to augment the ligand's redox potential values, yet to a lower extent than observed by Jouhara *et al.* However, more analysis is required to understand this, the lower amplitude redox potential shift can be accounted on the basis of different metal to ligand stoichiometries (1:3 versus 1:1, in this and Jouhara's work, respectively) as well as lower ionic potential of the used TMs.

When extending the CV scan window to higher potentials, an additional redox wave is measured at 1.25, 1.05, 0.06 and -0.60 V vs. Ag/Ag^+ corresponding to Ru^{2+}/Ru^{3+}, Fe^{2+}/Fe^{3+}, Co^{2+}/Co^{3+} and Mn^{2+}/Mn^{3+} redox couples, respectively. This firmly confirms the bipolar redox activity of these complexes, which could be advantageous for high specific capacity in battery cells. The observation of only two redox peaks for the ligand suggests that all carbonyl sites are reacting through a sequential 3 by 3 electrons process in the Phendi-TM complex. This observation is further evidenced by the amplitude of the redox current, which is almost 3 times higher than that for TM.

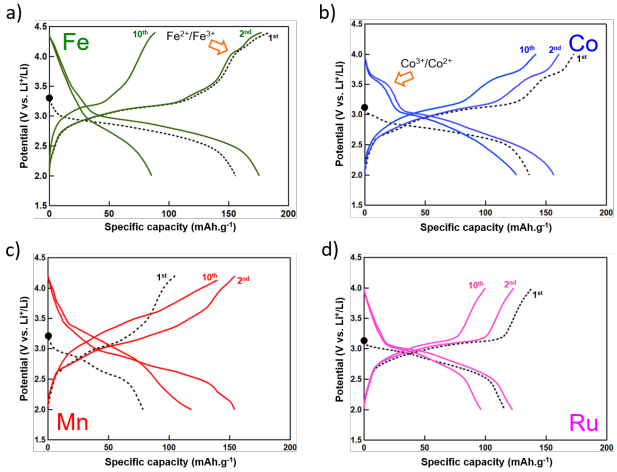

Figure 2. Typical potential-specific capacity traces displaying the 1st (black dashed line), 2nd and 10th cycles for Li half cells using $[TM(Phendi)_3]•2PF_6$ complexes as positive electrode (TM = Fe for (a) Co for (b), Mn for (c) and Ru for (d). The black dots indicate the OCV of the assembled cells.

The electrochemistry of the complexes was further evaluated in Li metal half-cells. Keeping in mind the solubility and stability factor of the Phendi-TM complexes, a high concentration electrolyte based on 5M LiTFSI/tetraglyme was found to be a suitable choice for cycling stability.[23] The potential-specific capacity profiles of the Phendi-TM complexes were studied at a typical cycling rate of 3 Li^+/e^- exchanged per formula unit of the complex in 10 hours (i.e., $3Li^+$/10h or C/20) (Figure 2). We deliberately selected to work at slow cycling rates to demonstrate the solubility effect of the chemical modifications applied. Such conditions remain more relevant as the dissolution, elution and diffusion of dissolved species processes are time dependent, and the common practice of fast cycling just simply translates into more cycles attained whereas test times remain of similar duration.

The OCV of the assembled cells was typically above 3.0 V vs. Li^+/Li for all the complexes (Figure 2). Since the ligands are in the oxidized state, all tests were started with a discharge (reduction) process. During the first discharge (dotted lines in Figure 2), only the carbonyl groups contribute to the charge storage; giving the full capacity (corresponding to 6 electrons exchange) for all the complexes, except Mn-based that delivered less capacity. During the following charge, the recovered capacity is considerably higher than the one delivered during the preceding discharge. This is due to the added activity of TM in the complexes (except for $[Ru(Phendi)_3]^{2+}$), which translates into higher practical energy as well. After the first cycle, all the complexes display reversible redox processes with equivalent capacity values. Note that higher capacity is delivered by $[Mn(Phendi)_3]^{2+}$ during the second cycle, which could be accounted on a percolation activation process at the first cycle. The complexes electrochemical behavior is characterized by a

sloped profile with an average operating potential around 3.0 V *vs*. Li^+/Li. In contrast with solution-based electrochemistry (Figure 1-c), the voltage profile is slightly different from the one for free Phendi where two distinguished plateaus at approximately 2.8 and 2.45 V vs. Li^+/Li are observed (Figure S4). This could be explained by the plausible clustering of Phendi ligands in the complex; a phenomenon which is commonly observed when switching from small molecule to polymers.[10b] Corroborating the molecular electrochemistry analysis (Fig. 1), the redox response of the ligand in the complexes evolve at higher potential than that of free PD.

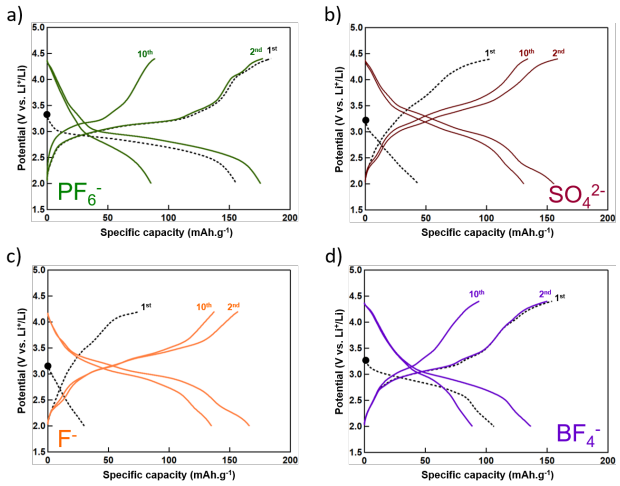

Figure 3. A typical potential-specific capacity traces showing the 1st (black dashed line), 2nd and 10th cycles for Li half cells using $[Fe(Phendi)_3]$•xA as positive electrode where A = PF_6^- for a), SO_4^{2-} for b), F^- for c) and BF_4^- for d). The black dots represent OCV of the assembled cells.

The preservation of the bipolar redox activity in solid-phase configuration is evidenced by the additional capacity attained at high potential (Figure 2). For instance, where the bipolar behavior is clearly visible, $[Co(Phendi)_3]^{2+}$ is exhibiting additional plateau at ~3.6 V vs. Li^+/Li corresponding to the redox of Co^{2+}/Co^{3+} (Figure 2b), which is also clearly seen in liquid configuration (Figure 1c). The same also applies for $[Fe(Phendi)_3]^{2+}$ where a pseudo-plateau is noticed at 4.1 V vs. Li^+/Li corresponding to the redox of Fe^{2+}/Fe^{3+}. For $[Mn(Phendi)_3]^{2+}$, the redox of Mn^{2+} overlaps with that of the ligand, since both are operating at close potentials also corroborating the molecular electrochemistry results (Figure 1-c). At this instance, an accurate estimation of the individual contribution from Fe/Mn is not feasible; significant difference in the 1st reduction and 1st oxidation capacities provides a direct and reasonable evidence. The bipolar behavior was not observed for $[Ru(Phendi)_3]^{2+}$ when tested in a similar potential window. This could simply be related to the fact that the redox potential of the Ru^{2+}/Ru^{3+} couple evolves at a higher potential and lies beyond the electrochemical stability window of the electrolyte used (as also noted in molecular electrochemistry analysis, Fig. 1c).

Regarding the cycling stability, the noticeable capacity loss after 10 cycles indicates that the as prepared complexes, with the PF_6^- counter-anions, remain intrinsically soluble in the used electrode design and electrolyte formulation. Marcilla *et al.,* have demonstrated that the solubility of polymerized ionic liquid can be tuned *via* an anion exchange reaction.[24] Similar effect was also noticed during the synthesis of the studied complexes: exchange of the Cl^- anions with PF_6^- in order to precipitate the complexes from water (refer to Experimental Section and SI). The reverse effect should be thus expected when working with non-aqueous electrolyte formulations. Thus, we have explored the impact of different anions on the cycling stability and indirectly on the solubility of the Phendi-TM complexes.

It should be noted that the anion exchange not only has profound effect on solubility of metal complexes but influences the overall molecular weight of the complex, leading also to higher theoretical capacities (for example, as high as 236 $mAh.g^{-1}$ could be attained for the $[Fe(Phendi)_3]$•2F complex; refer to Table S1). To provide deeper insights into the role of the counter-ion on solubility and hence electrochemical cyclability, a variety of anions were chosen judiciously. Keeping in mind the solubility of the respective Li salts ($LiPF_6$ and $LiBF_4$ being highly soluble, LiF with very limited, whereas Li_2SO_4 with no reported solubility in organic solvents), PF_6^-, BF_4^-, SO_4^{2-} and F^- were employed as counter-anions for charge compensation in the complex (refer to SI for synthesis and characterization details). Although similar qualitative results were obtained for the Co, Mn and Ru complexes, the discussion in the present study is limited to the $[Fe(Phendi)_3]$-based complex.

As observed with $[TM(Phendi)_3]$•$2PF_6$ (Figure 2), the galavanostatic cycling curves of $[Fe(Phendi)_3]$•xA also display different capacity values during the first discharge/charge processes, due to the additional redox activity of Fe^{2+}/Fe^{3+} couple. Note that less capacity is delivered for the complexes with F^- and SO_4^{2-} counter-ions. After that, efficient reversible electrochemical behavior with an average discharge potential of ~3.0 V vs. Li^+/Li is recorded, along with specific capacities ranging from 140 to 180 $mAh.g^{-1}$. As rationalized, the cycling stability of the Phendi-TM complexes was found strongly dependent on the anion chemistry (Figure 3). For example, a capacity retention of more than 80% was attained after 10 cycles for $[Fe(Phendi)_3]$•SO_4, whereas less than 50% was maintained for $[Fe(Phendi)_3]$•$2PF_6$ under similar conditions. Therefore, the capacity retention of $[Fe(Phendi)_3]^{2+}$ with different anions is following this order : SO_4^{2-} > F^- > BF_4^- > PF_6^-. As mentioned above, this follows the same trend as the respective Li salts, meaning that the anion-solvent interaction in both cases influences the solubility. The solubility is thus strongly dependent on the chemical nature of the anion, pointing out the existence of specific ionic interactions between the complex cation and different anions and solid stabilization towards solvation. As such, anionic substitution is an additional strategy to prevent the solubility and thus enhance the cycling stability of these complexes.

In summary, new multi-electron bipolar redox systems based on Phendi-TM complexes are being proposed for the first time as electrode for hybrid lithium batteries. First, we show that the redox potential of Phend-based complexes is impacted by the chemical nature of TM cation. The Phendi-TM complexes are additionally able to store energy by enabling the redox of both, ligands and TM center respectively. To further tune the solubility in battery electrolytes and improve the cycling

stability, anion substitution is found to be an efficient strategy. Future work can focus on design of more specific anions in order to completely suppress the solubility and increase the capacity. Moreover, whereas the intrinsically high solubility of the as made Phendi-TM complexes in battery electrolytes might be seen as a bottleneck for their utilization in solid phase batteries, it can be found advantageous for redox flow systems where to contrary, high solubility is being searched.

Experimental Section

Materials and general methods: Chemicals and solvents were purchased from commercial suppliers and used without further purification. $MnCl_2$, FeF_2 and $FeSO_4.7H_2O$ were purchased from Sigma Aldrich, NH_4PF_6 and NH_4BF_4 were purchased from Fluorochem, and $Ru(dmso)_4Cl_2$ was synthesized following a procedure described by Rempel *et al.* Lithium bis(trifluoromethane-sulfonym)imide (LiTFSI) and tetraglyme were purchased from TOB Energy. ^1H NMR and ^{13}C NMR spectra were recorded on a Bruker Avance II 300 spectrometer (at 300 and 75 MHz, respectively) at 298 K. Chemical shifts are given in ppm relative to TMS. Deuterated acetonitrile was purchased from Sigma Aldrich. Thermal analysis was performed on a Netzsch thermal analyser STA 449C Jupiter (heating rate: 10 °C.min^{-1} under nitrogen flow). Infrared spectra were recorded in ATR mode on a FTIR spectrometer at room temperature (Agilent). Spectra were measured over range of 4000 to 400 cm^{-1} with a resolution of 4 cm^{-1}.

Electrochemical analysis: All liquid CV measurements were performed in dry glove box under argon atmosphere and room temperature (O_2 and H_2O < 0.1 ppm). The electrolyte used is 0.1 M anhydrous acetonitrile (Sigma Aldrich), tetra-n-butyl-ammonium perchlorate (TBAP, Sigma Aldrich), were dried at 100 °C under vacuum and stored under argon atmosphere allowing to reach an amount of water in electrolyte less than 10 ppm. Cyclic voltammetry experiments were performed using a biologic SP-300 potentiostat/galvanostat equipped with a standard three electrodes electrochemical cell. Potentials were referred to an $Ag|AgClO_4$ 0.01 M reference electrode in 0.1 M TBAP/acetonitrile. The working electrode platinum disc (diam. 3 mm), was polished with 5, 2 and 1 µm diamond paste (MecaprexPresi), respectively. Platinum wire was used as a counter electrode. All CV experiments were repeated at least 3 times with fresh solutions. The battery performance of the complexes was tested vs. lithium in coin cells CR2032 using a Li metal disc as the negative electrode and fiber glass separators (Whatman) soaked with 5 M LiTFSI in Tetraglyme. The positive electrode was prepared in an argon-filled glovebox by grinding powder of complexes with 40% of carbon black (Ketjenblack EC-600JD) with pestle and mortar. The typical loading of the cells was 6-9 mg of active material. The cells were cycled in galvanostatic mode using BCS-805 in the potential range 2.0-4.4 V vs. Li^+/Li unless otherwise stated. A typical rate of three lithium ion exchanged per complex in 10 h was applied (i.e., 3 Li^+/10 h - C/20 ≡ cycling rate).

Acknowledgements

A.V. is indebted to the European Research Council (ERC) under the European Union's Horizon 2020 research and innovation program (grant agreement no. 770870). This work was partially supported by F.R.S.-FNRS under the grant agreement N° J.0111.16 - Equinox. S.D.K. and B.E. gratefully acknowledge the UCLouvain and the "*Prix Pierre et Colette Bauchau*" for financial support.

Conflict of Interest

The authors declare no conflict of interest.

Keywords: phendione-metal complexes • bipolar redox activity • organic electrode materials • lithium batteries

[1] a) R. C. Prince, P. Leslie Dutton, J. Malcolm Bruce, FEBS Letters 1983, 160, 273-276; b) T. Kogure, N. Wakisaka, H. Takaku, M. Takagi, Journal of Biotechnology 2007, 129, 502-509.

[2] a) J. Moiroux, D. Escourrou, M. B. Fleury, Electrochimica Acta 1980, 25, 785-790; b) G. Kokkinidis, D. Sazou, I. Moumtzis, Journal of Electroanalytical Chemistry and Interfacial Electrochemistry 1986, 213, 135-147.

[3] H. Alt, H. Binder, A. Köhling, G. Sandstede, Electrochimica Acta 1972, 17, 873-887.

[4] a) Q. Zhao, Z. Zhu, J. Chen, Advanced Materials 2017, 1607007; b) Y. Ding, C. Zhang, L. Zhang, Y. Zhou, G. Yu, Chemical Society Reviews 2018, 47, 69-103.

[5] a) A. E. Lakraychi, E. Deunf, K. Fahsi, P. Jimenez, J. P. Bonnet, F. Djedaini-Pilard, M. Bécuwe, P. Poizot, F. Dolhem, Journal of Materials Chemistry A 2018, 6, 19182-19189; b) Y. Lu, Q. Zhang, L. Li, Z. Niu, J. Chen, Chem 2018, 4, 2786-2813.

[6] Y. Liang, P. Zhang, S. Yang, Z. Tao, J. Chen, Advanced Energy Materials 2013, 3, 600-605.

[7] S. Gottis, A.-L. Barrès, F. Dolhem, P. Poizot, ACS Applied Materials & Interfaces 2014, 6, 10870-10876.

[8] a) S. Renault, S. Gottis, A.-L. Barres, M. Courty, O. Chauvet, F. Dolhem, P. Poizot, Energy & Environmental Science 2013, 6, 2124-2133; b) W. Wan, H. Lee, X. Yu, C. Wang, K.-W. Nam, X.-Q. Yang, H. Zhou, RSC Advances 2014, 4, 19878-19882; c) A. E. Lakraychi, K. Fahsi, L. Aymard, P. Poizot, F. Dolhem, J. P. Bonnet, Electrochemistry Communications 2017, 76, 47-50.

[9] L. Sieuw, A. Jouhara, É. Quarez, C. Auger, J.-F. Gohy, P. Poizot, A. Vlad, Chemical Science 2019, 10, 418-426.

[10] a) Z. Song, Y. Qian, X. Liu, T. Zhang, Y. Zhu, H. Yu, M. Otani, H. Zhou, Energy & Environmental Science 2014, 7, 4077-4086; b) Z. Song, H. Zhan, Y. Zhou, Chemical Communications 2009, 448-450; c) Z. Song, Y. Qian, M. L. Gordin, D. Tang, T. Xu, M. Otani, H. Zhan, H. Zhou, D. Wang, Angewandte Chemie International Edition 2015, 54, 13947-13951.

[11] a) Z. Lei, W. Wei-kun, W. An-bang, Y. Zhong-bao, C. Shi, Y. Yu-sheng, Journal of The Electrochemical Society 2011, 158, A991-A996; b) H. Li, W. Duan, Q. Zhao, F. Cheng, J. Liang, J. Chen, Inorganic Chemistry Frontiers 2014, 1, 193-199; c) Y. Liang, Z. Chen, Y. Jing, Y. Rong, A. Facchetti, Y. Yao, Journal of the American Chemical Society 2015, 137, 4956-4959; d) A. Vlad, K. Arnould, B. Ernould, L. Sieuw, J. Rolland, J.-F. Gohy, Journal of Materials Chemistry A 2015, 3, 11189-11193; eA. Jaffe, A. Saldivar Valdes, H. I. Karunadasa, Chemistry of Materials 2015, 27, 3568-3571.

[12] a) Z. Zhang, H. Yoshikawa, K. Awaga, Journal of the American Chemical Society 2014, 136, 16112-16115; b) F. Xu, S. Jin, H. Zhong, D. Wu, X. Yang, X. Chen, H. Wei, R. Fu, D. Jiang, Scientific Reports 2015, 5, 8225; c) Z. Zhang, H. Yoshikawa, K. Awaga,

Chemistry of Materials 2016, 28, 1298-1303; d) S. Wang, Q. Wang, P. Shao, Y. Han, X. Gao, L. Ma, S. Yuan, X. Ma, J. Zhou, X. Feng, B. Wang, Journal of the American Chemical Society 2017, 139, 4258-4261.

[13] a) C. Fang, Y. Huang, L. Yuan, Y. Liu, W. Chen, Y. Huang, K. Chen, J. Han, Q. Liu, Y. Huang, Angewandte Chemie International Edition 2017, 56, 6793-6797; b) P. Gao, Z. Chen, Z. Zhao-Karger, J. E. Mueller, C. Jung, S. Klyatskaya, T. Diemant, O. Fuhr, T. Jacob, R. J. Behm, M. Ruben, M. Fichtner, Angewandte Chemie International Edition 2017, 56, 10341-10346; c) Q. Zheng, Z. Niu, J. Ye, S. Zhang, L. Zhang, L. Li, Y. Zhao, X. Zhang, Advanced Functional Materials 2017, 27, 1604299; d) C.-H. Chang, A.-C. Li, I. Popovs, W. Kaveevivitchai, J.-L. Chen, K.-C. Chou, T.-S. Kuo, T.-H. Chen, Journal of Materials Chemistry A 2019, 7, 23770-23774.

[14] D. M. Boghaei, F. Behzadian Asl, Journal of Coordination Chemistry 2007, 60, 1629-1635.

[15] a) Q. Wu, M. Maskus, F. Pariente, F. Tobalina, V. M. Fernández, E. Lorenzo, H. D. Abruña, Analytical Chemistry 1996, 68, 3688-3696; b) G. Hilt, T. Jarbawi, W. R. Heineman, E. Steckhan, Chemistry – A European Journal 1997, 3, 79-88; c) S. Nehru, J. A. Anitha Priya, S. Hariharan, R. Vijay Solomon, S. Veeralakshmi, Journal of Biomolecular Structure and Dynamics 2019, 1-11; d) M. Q. Granato, D. d. S. Gonçalves, S. H. Seabra, M. McCann, M. Devereux, A. L. S. dos Santos, L. F. Kneipp, Frontiers in Microbiology 2017, 8.

[16] Y. Liang, P. Zhang, J. Chen, Chemical Science 2013, 4, 1330-1337.

[17] C. A. Goss, H. D. Abruna, Inorganic Chemistry 1985, 24, 4263-4267.

[18] L. Tong, Y. Jing, R. G. Gordon, M. J. Aziz, ACS Applied Energy Materials 2019, 2, 4016-4021.

[19] F. Calderazzo, F. Marchetti, G. Pampaloni, V. Passarelli, Journal of the Chemical Society, Dalton Transactions 1999, 4389-4396.

[20] F. Calderazzo, U. Englert, G. Pampaloni, U. Kölle, G. Tripepi, Journal of Organometallic Chemistry 1997, 543, 201-207.

[21] B. Elias, L. Herman, C. Moucheron, A. Kirsch-De Mesmaeker, Inorganic Chemistry 2007, 46, 4979-4988.

[22] A. Jouhara, N. Dupré, A.-C. Gaillot, D. Guyomard, F. Dolhem, P. Poizot, Nature Communications 2018, 9, 4401.

[23] K. Zhang, C. Guo, Q. Zhao, Z. Niu, J. Chen, Advanced Science 2015, 2, 1500018.

[24] R. Marcilla, J. Alberto Blazquez, J. Rodriguez, J. A. Pomposo, D. Mecerreyes, Journal of Polymer Science Part A: Polymer Chemistry 2004, 42, 208-212.

Supporting Information for

Biredox Phendione-Metal complexes as Electrode Materials for Lithium Batteries

Alae Eddine Lakraychi, Simon De Kreijger, Deepak Gupta, Benjamin Elias and Alexandru Vlad*

Supplementary tables

Table S1: Molecular weight and charge storage capacity values for Phendi-TM complexes studied in this work. In the formula oif the ionic potential, *n* is the charge and r is the ionic radius (in Å) of M. Theoretical capacities are calculated for 6 electrons exchange from Phendi carbonyls only.

	$[Mn(Phendi)_3].2PF_6$	$[Fe(Phendi)_3].2PF_6$	$[Co(Phendi)_3].2PF_6$	$[Ru(Phendi)_3].2PF_6$
Molecular weight ($g.mol^{-1}$)	1065.67	1066.56	1069.65	1111.79
Theoretical capacity ($mAh.g^{-1}$)	150.91	150.71	150.35	144.65
Specific capacity ($mAh.g^{-1}$)	160.50	170.22	158.19	138.12
Ionic potential of TM (n / r)	2.985	3.636	3.076	3.225

	$[Fe(Phendi)_3].SO_4$	$[Fe(Phendi)_3].2BF_4$	$[Fe(Phendi)_3].2F$
Molecular weight ($g.mol^{-1}$)	872.27	863.05	795.20
Theoretical capacity ($mAh.g^{-1}$)	184.27	186.36	202.25
Specific capacity ($mAh.g^{-1}$)	160.82	146.82	176.19

Synthetic procedures

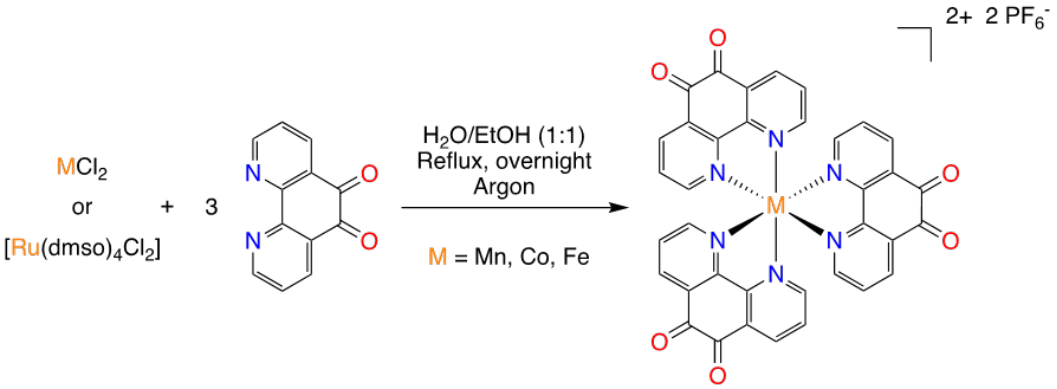

Scheme S1: Synthetic route of $[M(Phendi)_3].2PF_6$

$[M(Phendi)_3].2PF_6$: To a solution of MCl_2 (0.4 mmol) or $[Ru(dmso)_4Cl_2]$ (synthesized following a procedure described by Rempel et al.[1]) in water (20 ml) was added 1,10-phenantroline-5,6-dione (1.32 mmol, 277 mg) dissolved in 20 ml ethanol. The resulting solution was stirred overnight at room temperature under argon (and at reflux for the ruthenium complex). The solvents were removed, and the complex was recovered by the addition of a water saturated solution of hexafluorophosphate (NH_4PF_6). The product, $[M(Phendi)_3].2PF_6$, was collected by centrifugation and washed with cold water (three times), ethanol (two times) and diethylether (three times), and then dried under vacuum. Yields: 325 mg, 83% ($[Co(Phendi)_3].2PF_6$); 280 mg, 72% ($[Mn(Phendi)_3].2PF_6$); 351mg, 90% ($[Fe(Phendi)_3].2PF_6$); 278 mg, 66% ($[Ru(Phendi)_3].2PF_6$).

$[Fe(Phendi)_3].2PF_6$: ^{1}H NMR (300 MHz, CD_3CN) δ (ppm) 8.65 (dd, J = 7.9, 1.3 Hz, 1H), 7.82 (dd, J = 5.6, 1.4 Hz, 1H), 7.72 (dd, J = 7.9, 5.6 Hz, 1H)

$[Fe(Phendi)_3].2PF_6$: ^{13}C NMR (75 MHz, CD_3CN) δ (ppm) 129.85, 131.71, 138.62, 159.06, 160.69, 175.91 (C=O)

$[Ru(Phendi)_3].2PF_6$: ^{1}H NMR (300 MHz, CD_3CN) δ (ppm) 9.05 (dd, J = 4.7, 1.8 Hz, 1H), 8.44 (dd, J = 7.9, 1.8 Hz, 1H), 7.64 (dd, J = 7.9, 4.7 Hz, 1H).

$[Fe(Phendi)_3].2PF_6$: ^{1}H NMR (300 MHz, CD_3CN) δ (ppm) 129.92, 131.78, 137.85, 157.15, 158.05, 175.95 (C=O)

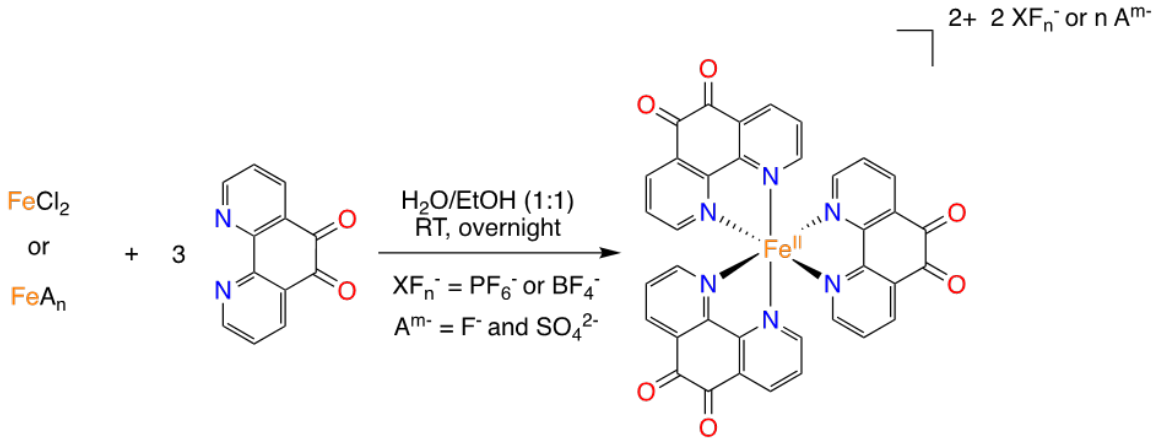

Scheme S2: Synthetic route of $[Fe(Phendi)_3].xAnion$

$[Fe(Phendi)_3].xAnion$: To a solution of $FeCl_2$ (0.4 mmol) in water (20 ml) was added 1,10-phenantroline-5,6-dione (1.32 mmol, 277 mg) dissolved in 20 ml of ethanol. The resulting solution was stirred overnight at room temperature under argon. The solvents were removed, and the complex was recovered by the addition of a water saturated solution of the corresponding ammonium salt (NH_4BF_4 or NH_4PF_6). The product, $[Fe(Phendi)_3].2F_n$, was collected by centrifugation and washed with cold water (three times), ethanol (two times) and diethylether (three times), and then dried under vacuum. Yields: 351mg, 90% ($[Fe(Phendi)_3].2PF_6$); 254 mg, 74% ($[Fe(Phendi)_3].2BF_4$). To a solution of FeF_2 or $FeSO_4.7H_2O$ (0.4 mmol) in water (20 ml) was added 1,10-phenantroline-5,6-dione (1.32 mmol, 277 mg) dissolved in 20 ml of ethanol. The resulting solution was stirred overnight at room temperature under argon. The solvents were removed, and the complex was washed three times with dimethyl carbonate. The product, $[Fe(Phendi)_3].nA$ was then dried under vacuum. Yields: 145 mg, 50% ($[Fe(Phendi)_3].2F$); 240 mg, 68% ($[Fe(Phendi)_3]SO_4$.

Complementary characterizations

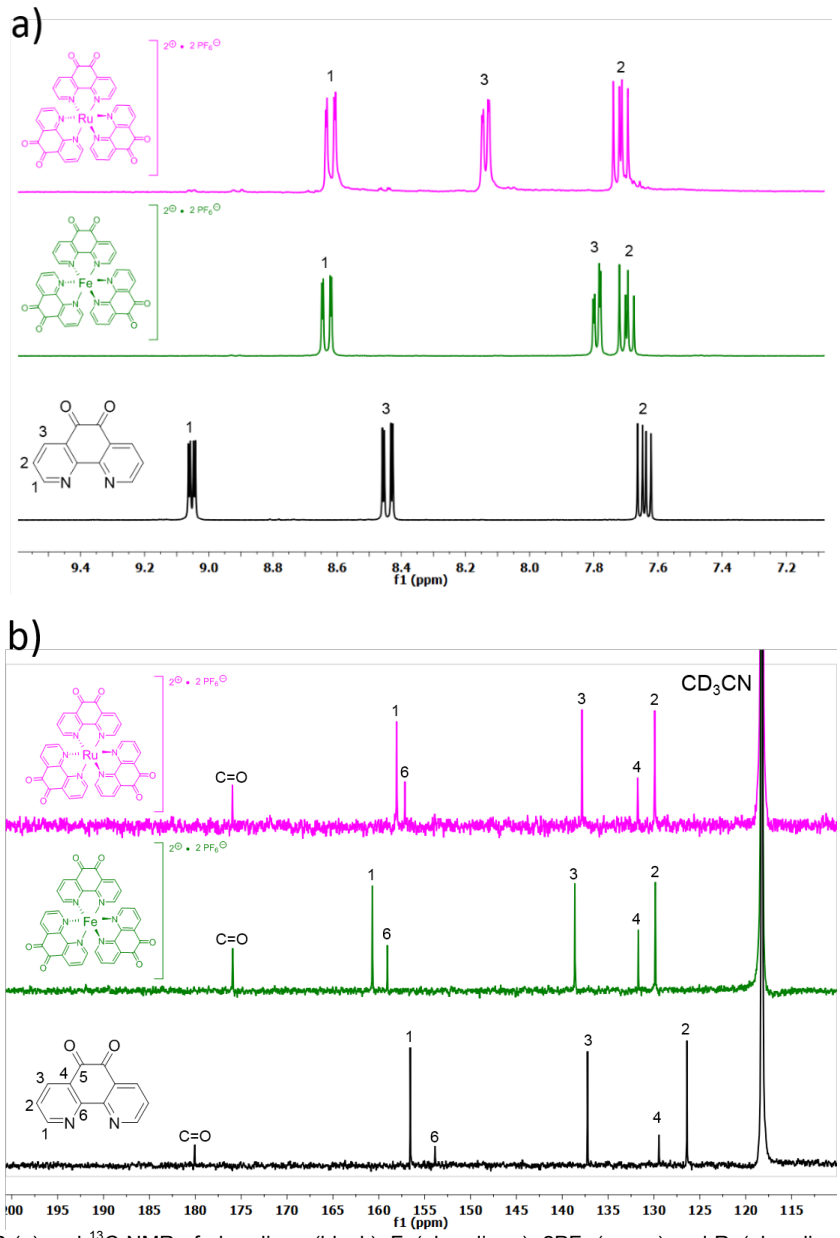

Figure S1: Typical ^{1}H NMR (a) and ^{13}C NMR of phendione (black), Fe(phendione)$_3$.2PF$_6$ (green) and Ru(phendione)$_3$.2PF$_6$ (pink) measured in CD_3CN at 300 and 75 MHz respectively.

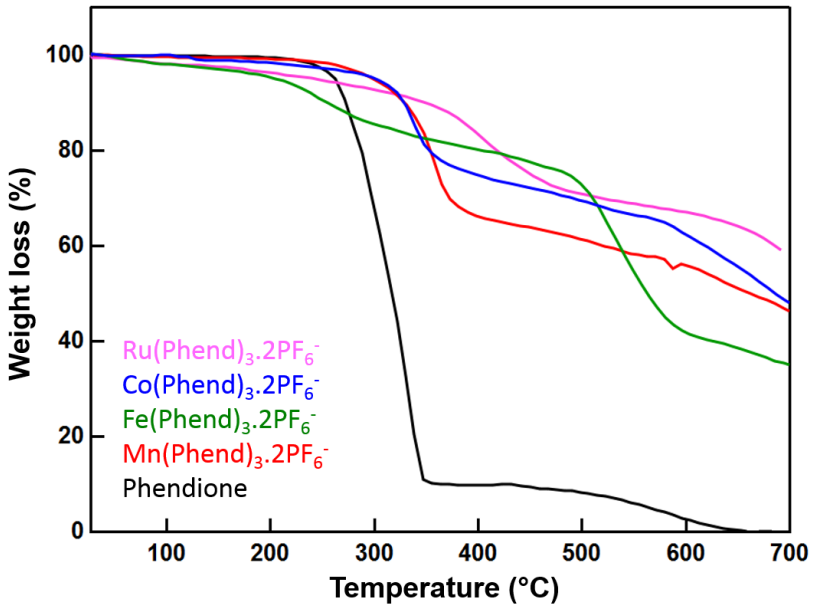

Figure S2: Thermogravimetric (TG) traces of phendione and phendione complexes obtained under nitrogen at a heating rate of 10 °C.min^{-1}.

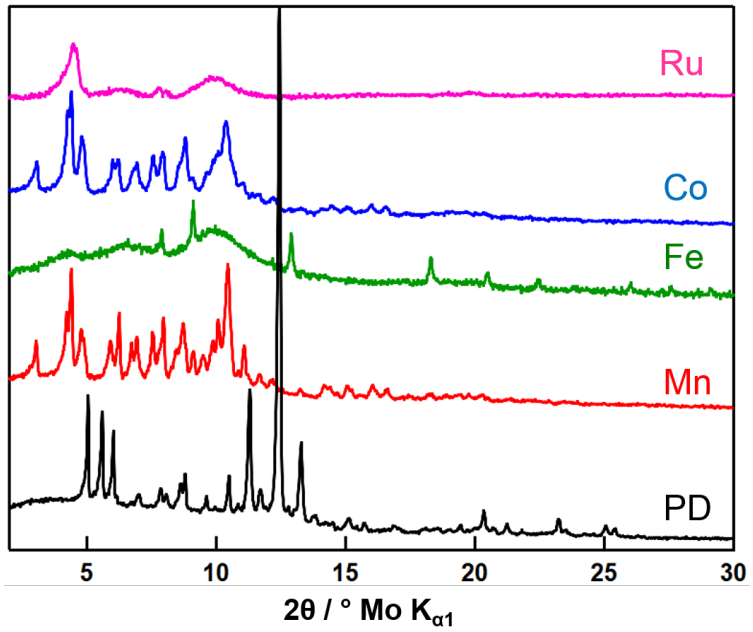

Figure S3: PXRD patterns of Phendi and [M(Phendi)3.2PF6] complexes (M : Mn, Fe, Co and Ru).

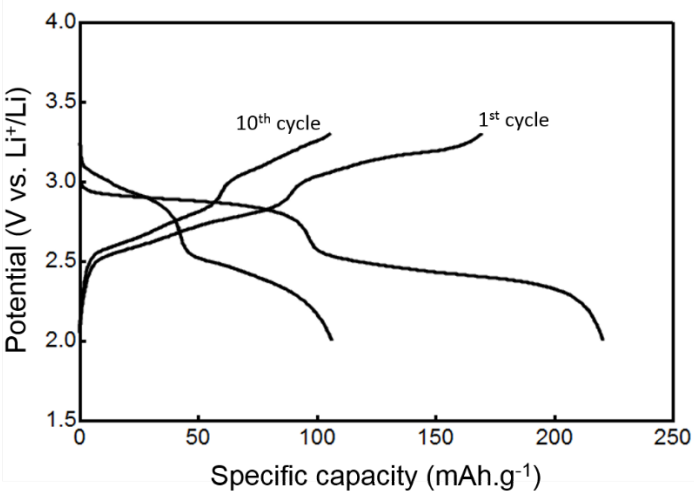

Figure S4: A typical potential-specific capacity traces showing the 1st and 10th cycles for Li half-cell using free phendione as positive electrode in 5 M LiTFSI/tertraglyme. The C-rate was 1 Li^+/10h ≡ C/20.

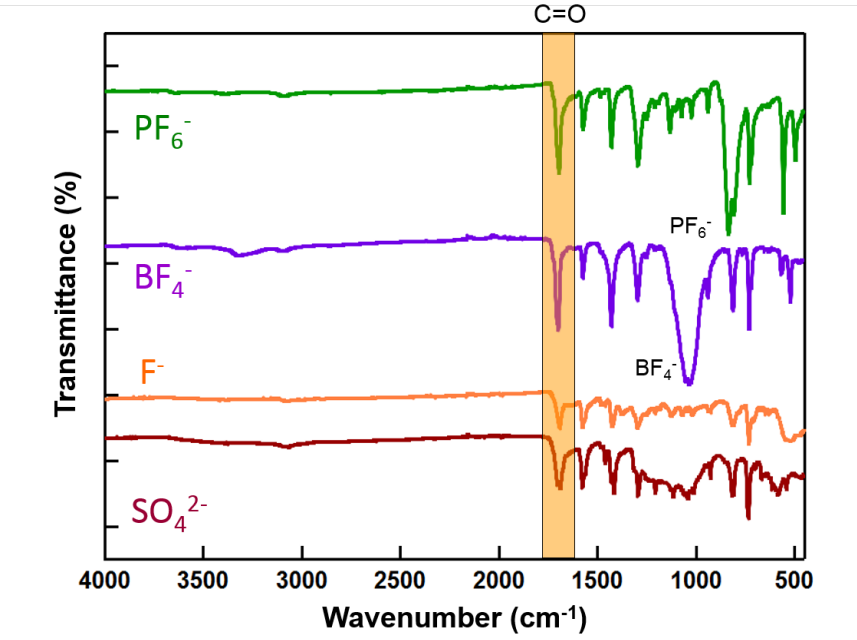

Figure S5: Overlaid FTIR spectra of $[Fe(phendione)_3]^{2+}$ with SO_4^{2-} (brown), F^- (orange), BF_4^- (purple) and PF_6^- (green). Spectra were recorded on ATR mode.

The complex cation $[Fe(phendione)_3]^{2+}$ is showing the carbonyl bond at exactly the same wavenumner (1720 cm^{-1}) whatever the anion used. This value remains higher than the one observed for free phendione (1720 cm^{-1}) indicating the complexation has taken place for all the anions. Note that the PF_6^- and BF_4^- are appearing at 848 and 1052 cm^{-1} respectively.

References

[1] B.R. James, E. OChiai, and G.I. Rempel, Inorg. Nuclear Chem. Letters, 1971, 7, 781.